Highly accumulated electron layer at a semiconductor/electrolyte interface

A. Tardella* and J.-N. Chazalviel
Laboratoire de Physique de la Matière Condensée,† Ecole Polytechnique, F-91128 Palaiseau, France
(Received 8 February 1985)

We present studies on accumulated electron layers realized on the silicon/acetonitrile interface at room temperature. This interface has a behavior qualitatively similar to that of the Si/SiO_2 interface, but has allowed us to observe electron densities as high as 8×10^{13} cm^{-2}. The interface is realized in an electrochemical cell, and electric measurements are performed with a three-electrode arrangement. The electron density is determined by capacitance-voltage measurements. Conductivity measurements allow determination of the mean scattering time of the two-dimensional electron gas, which can be as short as 10^{-14} s. The special sample design also allows one to perform infrared-absorption measurements of the interface, in the (1.1—10)-μm region, using the attenuated-total-reflection-spectroscopy technique. This absorption is about 4% per reflection at 10 μm and varies as $\omega^{-3/2}$. We have extended the existing theory to the case of highly concentrated accumulation layers and we find a satisfactory agreement with our experimental results. The comparison between theory and experiment allows one to deduce a value of 0.22 F m^{-2} for the capacitance of the Helmholtz layer and a flat-band potential in good agreement with that determined from a Schottky-Mott plot. The mobility of electrons in the accumulation layer is determined as a function of electron density. It varies as $\sim n_s^{-1/2}$ at very high concentrations. From comparison with earlier works, it can be inferred that phonon scattering is the limiting mechanism for the mobility at high accumulations, and can account for the magnitude and the $\omega^{-3/2}$ dependence of the optical absorption.

I. INTRODUCTION

Many theoretical and experimental studies have been realized on metal-oxide-semiconductor (MOS) structures, starting in the 1950s, because of their technological and fundamental interest. The MOS structure allows two-dimensional carrier systems to be realized, with voltage-controlled densities. Ando, Fowler, and Stern have published an important synthesis on these two-dimensional systems.[1] However, because of dielectric breakdown, the carrier density is limited to 2×10^{13} cm^{-2}. We present experiments on a two-dimensional electron gas with voltage-controlled densities approaching 10^{14} cm^{-2}, at room temperature, using a semiconductor/electrolyte interface. With this interface, carrier density is only limited by the voltage of electrolyte decomposition. Using a nonaqueous solvent (such as acetonitrile), this voltage may reach 3 V. Then the electric field at the semiconductor surface can be higher than in MOS structures. These investigations were performed using (i) capacitance measurements, (ii) conductivity measurements, and (iii) infrared-absorption measurements. In Sec. II we recall some generalities on the semiconductor/electrolyte interface. In Sec. III we describe the experimental arrangement. The experimental results are presented in Sec. IV. In Sec. V we present the theory of very high accumulation layers. The theoretical and experimental results are compared and discussed in Sec. VI.

II. SEMICONDUCTOR/ELECTROLYTE INTERFACE

The electronic properties of semiconductors can be described by band theory. For the case of electrolytes, band theory does not apply; however, a few similarities can be found.

We consider an acetonitrile (ACN) + 0.1M tetrabutylammonium perchlorate (TBAP) solution. *Occupied* electronic levels are present in this solution corresponding to various chemical bonds. Under certain potential conditions, some of these levels can be emptied by breaking of the associated chemical bonds: This corresponds to the *anodic* decomposition of the electrolyte. These levels are similar to the valence band of a semiconductor. *Empty* levels are also present in the solution, that can be filled under certain potential conditions, by breaking of other chemical bonds. This corresponds to the *cathodic* decomposition of the electrolyte. These latter levels are similar to the conduction band of a semiconductor. Between these two series of levels, separated by about 5 eV,[2] and in the absence of redox species in the solution, there are no allowed electronic levels: this is similar to the forbidden gap of a semiconductor. If redox (oxidizable or reducible) species are present in the solution, they create levels that can be regarded as donors in the reduced form and acceptors in the oxidized form. For the reaction

$$A(\text{ox})+ne^-\rightarrow D(\text{red}),$$

and if both forms coexist in the solution, the chemical potential for the electrons is given by the Nernst formula:

$$\mu=\mu_0+(kT/ne)\ln\{[D(\text{red})]/[A(\text{ox})]\}.$$

Practically, there are always impurities in the solution such as water in acetonitrile that create a few levels in the "forbidden gap" of the electrolyte.

When the interface is realized, the chemical potentials for the electrons in the semiconductor and in the electro-

lyte must equalize at equilibrium. The bands of the semiconductor bend and a layer of ionic charge arises in the electrolyte. In the absence of surface states, this charge density is opposed to the space-charge density in the semiconductor (the equilibrium conditions are modified by the presence of surface states). The region between the electrode surface and the ionic layer is called the Helmholtz layer. A voltage generally exists between the semiconductor and the electrolyte, at equilibrium.

An extra voltage can be applied to the interface by using a reference electrode whose potential relative to the solution is fixed. We used an Ag/Ag^+ reference electrode whose redox potential lies in the forbidden gap of silicon [Fig. 1(a)].[3]

In the following we will use the standard electrochemical convention, i.e., the "electrode potential" V is the potential of the silicon sample relative to the reference electrode, whereas the "gate voltage" used for MOS structures corresponds to the opposite convention. For $V=0$ the Fermi level in the silicon and the redox level of the Ag/Ag^+ couple are equal [Fig. 1(b)]. A depletion layer exists in the silicon. For an applied electrode potential V, two qualitatively different situations can occur depending upon whether or not redox species exist in the solution in a concentration sufficient to accommodate all the electrons that may cross the interface. If the above condition is fulfilled, the junction behaves just as a metal/semiconductor interface.

We are interested in the opposite case, where the only redox species in the solution are low concentrated impurities. For $V>0$ the depletion layer is thicker than that shown in Fig. 1(b). A very weak current flows through the interface, due to the impurities in the solution, but is limited by electron transfer over the Schottky barrier. On the other hand, for $0>V>-3$ V, only a weak current can flow through the interface due to the impurities, but it is limited by the impurity diffusion in the solution. The electrolyte and the silicon, being conductors, have equipotential volumes. Hence the potential drop occurs at the interface, divided between the space-charge region in the semiconductor and the Helmholtz layer in the electrolyte, according to their capacitances. For $0>V>V_{FB}$ (flat-band potential), almost the whole potential drop is in the silicon, and the bands become increasingly flat. For $V<V_{FB}$, the bands bend downward and an accumulation layer appears. Figure 1(c) shows the band bending for $V=V_C$ (conduction-band potential). Beyond this latter situation, the accumulation layer is degenerate [Fig. 1(d)] and its charge density becomes very high with thickness comparable to the thickness of the Helmholtz layer. The accumulation layer capacitance in this case becomes comparable to the Helmholtz-layer capacitance; hence the potential drop across the Helmholtz layer is no longer negligible.

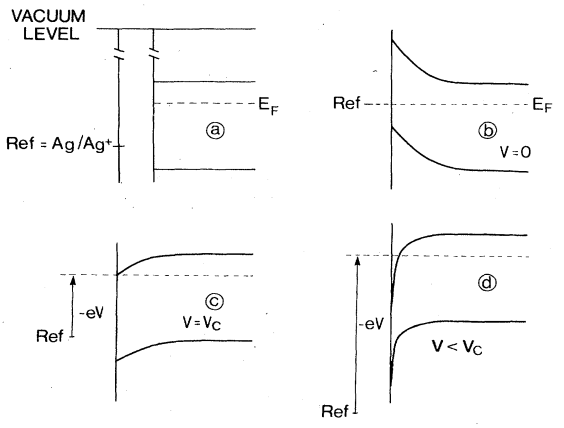

FIG. 1. Band schematic in various situations. (a) Relative positions, in the absence of charges, of the forbidden gap of silicon, of the Fermi level corresponding to 2.5×10^{15} donors per cm^3 at room temperature, and of the potential of the redox couple $Ag/10^{-2}M$ Ag^+. Also shown are band bendings corresponding to (b) zero electrode potential, (c) the conduction-band potential, and (d) degenerated accumulation layer.

III. EXPERIMENT

The silicon sample was cut from an n-type (111)-oriented silicon monocrystalline ingot of ~3 Ω cm resistivity. Figure 2 shows the silicon sample and its holder. This special design allows (i) optical measurements by using attenuated total-reflection spectroscopy,[4] and (ii) protection of the face with the prisms and the Ohmic contacts (backface) from the corrosive solution used for polishing the face to be exposed to the electrolyte (front face). The sample was roughed out with a diamond saw. The back face was machined with a diamond mill. The faces of the prisms and the bottom of the back face were optically polished by hand. The front face was first mechanically polished after sawing and then mechanochemically polished using a solution of $Cu(NO_3)_2$ and NH_4F.[5] The final thickness of the sample is 1.35 mm and the separation between the prisms is 8 mm. The angle between the polished faces of the prisms and the plane of the interface is 45°.

The junction was realized in the electrochemical cell, whose schematic is presented as Fig. 3. The electrochemical measurements were performed with a three-electrode arrangement and a potentiostat.[6] The working electrode W is the silicon sample. The area exposed to the electro-

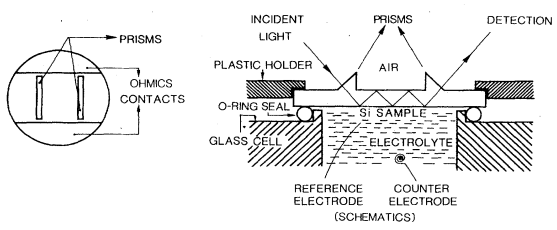

FIG. 2. Sample mounting: This allows electrochemical measurements, conductivity measurements, and optical measurements using attenuated-total-reflection spectroscopy.

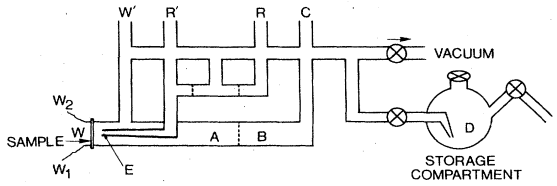

FIG. 3. Schematic of the electrochemical cell. *A*, working electrode compartment; *B*, counter electrode compartment; *D*, storage compartment; *E*, tapered pipe; *W*, working electrode; W_1, W_2, Ohmic contacts; *W'*, second working electrode; *R*,*R'*, two possibilities of reference electrodes; *C*, counter electrode.

lyte is 2.4 cm^2. The reference electrode *R* is a Ag wire immersed in a Ag^+ solution. The counter electrode *C* is a platinum wire. This arrangement allows current-voltage and impedance-voltage measurements. However, an experimental difficulty arose at the larger frequencies from the high values of the silicon/acetonitrile interface capacitance (up to 15 μF) and the series resistance of the reference electrode ($\sim 10^5$ Ω). This problem has been solved by introducing a platinum wire *R'* close to the silicon surface, connected to *R* through a 200 μF capacitance. The electrolyte was acetonitrile (ACN) + 0.1*M* TBAP. Acetonitrile, a Merck Uvasol-grade product, was left standing for 1 d on molecular sieves, then out-gassed through freeze-pump-thaw cycles, and finally vacuum-distilled and stored under vacuum on activated molecular sieves. TBAP was dried under vacuum by heating at ~ 50 °C for several hours. The solution was prepared by vacuum distillation of ~ 30 cm^3 ACN on TBAP in the storage compartment. Before each experiment, the front face of the silicon sample was rinsed with 40% hydrofluoric acid solution. The experimental arrangement used for the optical measurements is shown in Fig. 4. We used a Perkin-Elmer monochromator with two blazed gratings. The infrared source was a Nernst glower. Two detectors

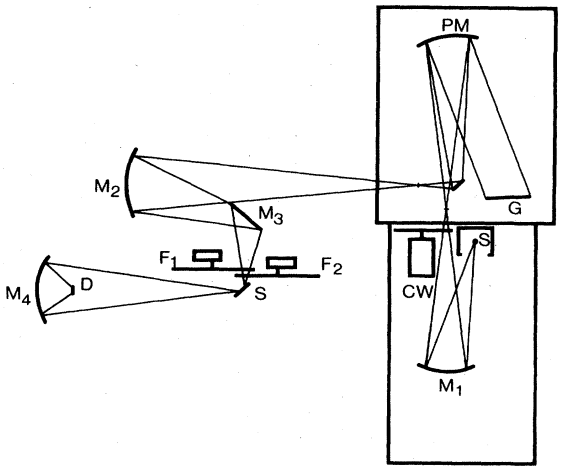

FIG. 4. General experimental arrangement. *S*, light source (Nernst glower); CW, chopper wheel; *G*, gratings; PM, parabolic mirror; M_1, M_2, M_4, spherical mirrors; M_3, plane mirror; F_1, F_2, movable filters; *S*, sample location (cell not represented); *D*, detector.

have been used: a pyroelectric detector from Eltec, used at a modulation frequency of 20 Hz and an InSb photovoltaic detector from Infrared Associates, used at a modulation frequency of 70 Hz. The electric signal from the potentiostat or the detectors was fed to a Thomson THN600 lock-in amplifier. The spectral region is limited at short wavelength to 1.1 μm by the band-gap absorption and at long wavelength to 10 μm by the lattice absorption of silicon.[7] Nonpolarized and polarized light were used (linear polarization either parallel to the interface, *s* polarization; or perpendicular to the precedent one, *p* polarization). The geometry of the sample allows four useful reflections on the silicon/acetonitrile interface. Classical transmission measurements have been performed by mechanically chopping the light beam. Electrode potential modulation with the help of the potentiostat allows measurement of electromodulated spectra. The relative absorption of the interface is given by the ratio of an electromodulated spectrum to a classical transmission spectrum. This computation together with data acquisition and control of the switching between the various measurements was performed by a Commodore CBM3016 microcomputer via an IEEE-488 bus.

IV. RESULTS

The admittance-frequency curves have been investigated between 7 and 2000 Hz. For typical accumulations and up to 200 Hz, the interface is equivalent to a capacitance $C \sim 10$ μF. At higher frequencies the series resistance $R \sim 20$ Ω appears. Routine admittance-voltage measurements were therefore performed at a modulation frequency of 20 Hz so that the imaginary part of the admittance is directly proportional to the capacitance of the interface. Figure 5 shows (a) the imaginary part (capacitance) of the admittance, (b) the real part of the admittance, and (c) the *I-V* curve (voltammogram) measured on a freshly prepared junction. These three curves were realized within 3 min. We can see that the leaking currents due to water in the solution are very weak for $V > -2.5$ V and that the small associated peaks near $V = -2.5$ V do not hinder the capacitance-voltage measurements (*C-V*). The peak near $V = -0.5$ V on the *C-V* curve is known to be characteristic of surface states.[8] Electron densities n_s in the accumulation layer as high as 8×10^{13} cm^{-2} were deduced by integrating the *C-V* curves. We observed an evolution of this number. Typically, an initial electron density of $\sim 7 \times 10^{13}$ cm^{-2} falls to $\sim 5 \times 10^{13}$ cm^{-2} 3 h later and becomes 4×10^{13} cm^{-2} after 1 d. In the same time the estimation of the surface-state density by integrating the peak at $V \sim -0.5$ V evolves from 2×10^{12} to 5×10^{12} cm^{-2}. This density always stays much smaller than n_s.

Figure 5(d) shows the conductivity σ_{acc} of the accumulation layer versus electrode potential. σ_{acc} was deduced by measuring the variation of resistance *R* of the sample between the two contacts W_1 and W_2 (see Fig. 3). We have

$$\sigma_{acc} = g[1/R(V) - 1/R(0)] ,$$

with $R(0) = 13.5$ Ω. The geometrical factor *g* was mea-

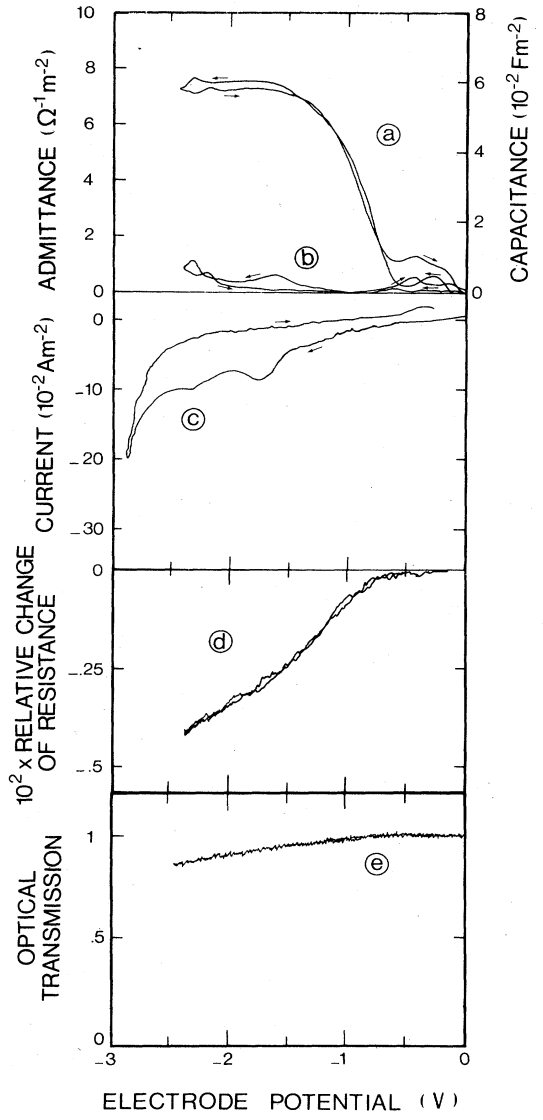

FIG. 5. Experimental results on the (111) *n*-silicon/acetonitrile interface as a function of electrode potential. (a) Imaginary and (b) real parts of the admittance measured at 20 Hz frequency; (c) electrochemical current density (voltammogram); (d) relative change of resistance of the sample between the two Ohmic contacts W_1 and W_2 (see Fig. 2) measured at 20 Hz frequency; (e) optical transmission for four reflections at the wavelength of 8.13 μm (1230 cm^{-1}) measured with the light beam mechanically chopped at 20 Hz frequency.

sured by analog simulation. The silicon sample and the accumulation layer were simulated with a negative mold, machined to scale 5, filled with salt water, in which the liquid level could be changed. We found $g=1.4$. The measurement of $R(V)$ was performed at 20 Hz. Special attention was paid to the unwanted effects that might arise from the conduction through the interface and the electrolyte. For the curve shown in Fig. 5(d), the contribution of these effects amounts to at most the noise level.

Figure 5(e) shows the transmission of the sample versus

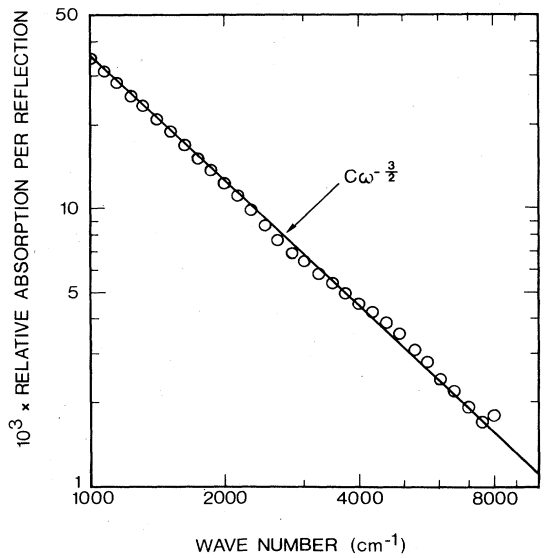

FIG. 6. Relative absorption per reflection of *s*-polarized light at the (111) *n*-silicon/acetonitrile interface vs wave number $1/\lambda=\omega/2\pi c$. The straight line represents a $\omega^{-3/2}$ dependence.

electrode potential for a freshly prepared interface, at a wavelength of 8.13 μm ($1/\lambda=1230$ cm^{-1}). For $V=-2.5$ V, 15% of the incident light beam is absorbed in the accumulation layer, i.e., 3.75% per reflection. Figure 6 shows the relative absorption A_s per reflection of the interface versus wave number $1/\lambda$. This curve is featureless and A_s varies as $\sim\lambda^{3/2}$. Absolute calibration of the relative absorption—wave-number curves has been made with a transmission-voltage measurement. As recording one spectrum takes about 20 min, we have verified that the surface does not evolve during the data acquisition, by doing a *C-V* measurement before and after each spectrum. Figure 6 corresponds to $n_s=5.4\times10^{13}$ cm^{-2}. Curves of relative absorption A_p per reflection with *p*-polarized light have also been determined. $A_s(1/\lambda)$ and $A_p(1/\lambda)$ are found to be proportional to each other with $A_s/A_p\sim1.1$. The relevance of the A_s/A_p ratio will be discussed in Sec. VI C.

V. THEORY OF THE ACCUMULATION LAYER

Theoretical studies on accumulation and inversion layers have been made for a long time. However, no theoretical results are available on accumulation layers for electron densities above 1.5×10^{13} cm^{-2}. Thus we extend the method exposed in Ando to higher densities.[9] We consider an *n*-type (111)-oriented silicon crystal lying in the half-space $z>0$. All the relevant physical quantities depend on z only. We have performed the calculation corresponding to our experimental conditions (temperature $T=300$ K, donor density $N_D=2\times10^{15}$ cm^{-3}), but the results in the degenerate accumulation regime are thought to be rather insensitive to these parameters. In our case the Fermi level E_F lies 250 meV below the bottom of the bulk conduction band. In the space-charge region, near the interface, the band bending is described by

the Hartree potential $V_H(z)$. At the interface, the Hartree potential takes the value $V_s = V_H(0)$. We want to calculate the electron density n_s and $V_H(z)$ as a function of V_s. The motion of the electrons in the accumulation layer is quantized and the envelope function $\zeta_i(z)$ in the effective-mass approximation satisfies

$$\frac{\hbar^2}{2m_z}\frac{d^2\zeta_i(z)}{dz^2}+[E_i-V(z)]\zeta_i(z)=0 ,$$

with $V(z)=V_H(z)+V_I(z)$, E_i is the energy of the ith subband, $V_I(z)$ is image potential, $m_z=3m_t m_l/(m_t+2m_l)$, and[10] $m_t=0.19m_e, m_l=0.97m_e$.

$\zeta_i(z)$ must be normalized to 1 and go to 0 for $z\to\infty$ and $z=0$. This latter condition corresponds to the nonpenetration of the wave function into the electrolyte. In addition, $V_H(z)$ is linked to the functions $\zeta_i(z)$ through the electrostatic potential $\phi(z)=V_H(z)/(-e)$ and Poisson's equation:

$$\frac{\partial^2\phi(z)}{\partial z^2}+\frac{\rho(z)}{\epsilon_0\epsilon_r}=0 ,$$

where $\rho(z)$ is the total charge density, $\rho(z)=\sum_i \rho_i(z)+\rho_d(z)$, with $\rho_i(z)$ the contribution of the ith subband and $\rho_d(z)$ the contribution of the ionized donors.

We have

$$\rho_i(z)=|\zeta_i(z)|^2\int_{E_i}^{\infty} D_i(E)f(E)dE ,$$

where $D_i(E)$ is the two-dimensional density of states:[11]

$$D_i(E)=g_v m_d/\pi\hbar^2 \quad \text{for } E>E_i ,$$

$$D_i(E)=0 \quad \text{for } E<E_i ,$$

and g_v is the valley degeneracy (6 in our case[9]) and m_d is the density-of-states effective mass ($m_d=[m_t(m_t+2m_l)/3]^{1/2}$ in our case).

The energies E_i, the wave functions $\zeta_i(z)$, and the Hartree potentials $V_H(z)$ were calculated by a self-consistent method for each value of V_s. Several kinds of results can be presented.

Figure 7 shows the first five energy levels, the electron density n_s, and the capacitance $C_A=e\,dn_s/dV_s$ of the accumulation layer versus V_s. In these calculations V_s is referenced to E_F. Figure 8(a) shows the self-consistent

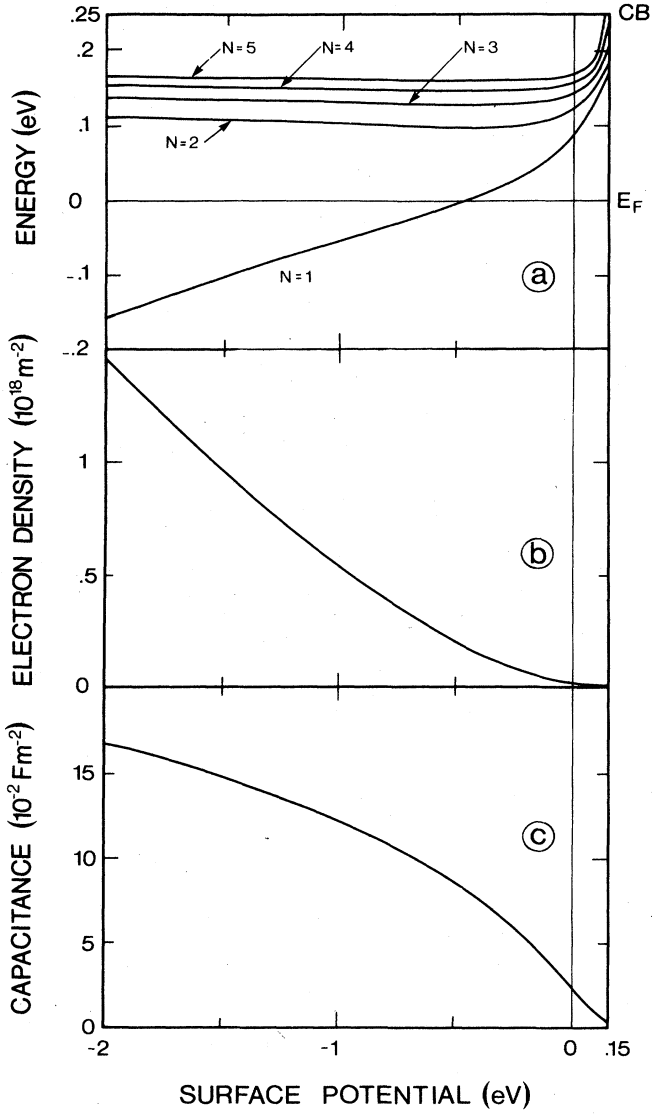

FIG. 7. Calculated results for a highly accumulated layer on (111) n-silicon vs surface Hartree potential. Energies are referenced to the bulk Fermi level. (a) Energies of the five lowest subband minima; CB, bulk conduction-band minimum; E_F, Fermi level. (b) Electron density. (c) Capacitance.

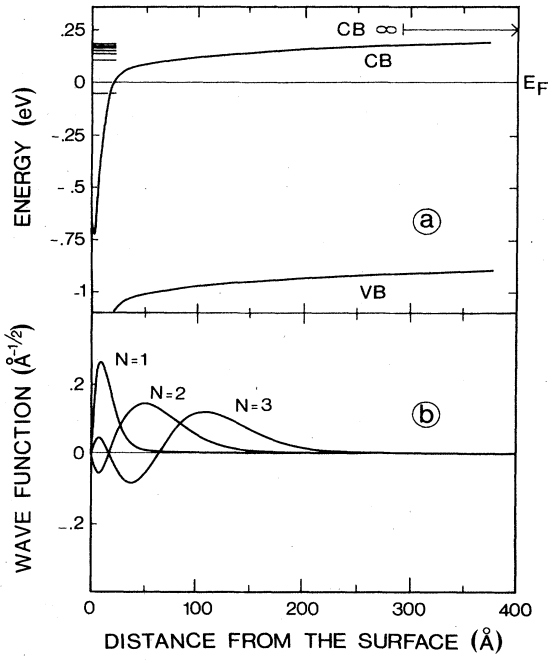

FIG. 8. Calculated results vs distance from the surface for an accumulation layer on (111) n-silicon and a surface Hartree potential of -1 eV. Energies are referenced to the bulk Fermi level. (a) Self-consistent potential. The dashes on the energy axis represent the seven lowest subband minima. VB, valence band; CB, conduction band; CB∞, bulk conduction-band minimum; E_F, Fermi level. (b) Envelope function of the wave function for the three lowest subbands.

potential $V(z)$ and energy levels for $V_s - E_F = -1$ eV. The associated first three wave functions are shown in Fig. 8(b). We have $n_s = 5.27 \times 10^{13}$ cm^{-2}. $V(z)$ crosses the Fermi level at ~ 20 Å from the surface, falls down to a minimum at 6 Å and rises near the surface because of the image potential. The first energy level lies 52.8 meV below the Fermi level, the difference between the first two levels is 152 meV, and 98% of the electrons are confined in the first subband. The average distance of the electrons from the surface in this subband is 12.85 Å.

VI. DISCUSSION

A. Electron density in the accumulation layer

The results given in the preceding section apply to the silicon side of the interface. In order to calculate the capacitance of the interface versus electrode potential and compare it with the experimental results, we must make allowance for the electrolyte side of the interface. A calculation similar to the preceding one should be done, but this is a very difficult theoretical problem. Therefore we used simplifying hypotheses. They consist of (i) neglecting the effects of surface states, and (ii) treating the electrolyte side of the interface as an unknown series capacitance, independent of electrode potential. Under these conditions, the capacitance C_I of the interface is merely

$$\frac{1}{C_I(V_I)} = \frac{1}{C_A(V_A)} + \frac{1}{C_H(V_H)} ,$$

where V_A is the potential drop in the accumulation layer, V_H is the potential drop in the Helmholtz layer, and $V_I = V_A + V_H$ is the total potential drop through the interface. C_A is the capacitance of the accumulation layer, and C_H is the capacitance of the Helmholtz layer.

According to the second hypothesis, we have $V_H = Q_A(V_H)/C_H$, where Q_A is the accumulated charge in silicon. The calculations presented in Sec. V give $Q_A(V_A)$ and $C_A(V_A)$, so that the relation $C_I(V_I)$ is parametrized by V_A:

$$C_I = \frac{C_H C_A(V_A)}{C_H + C_A(V_A)}, \quad V_I = V_A + \frac{Q_A(V_A)}{C_H} .$$

We see that V_I is 0 when V_A is 0, i.e., for the flat-band potential V_{FB}. Hence, the potential scale for the calculated $C_I(V_I)$ curve is relative to V_{FB}. On the other hand, the potential scale for the experimental $C(V)$ curves is relative to the reference potential. Then in order to compare experimental and calculated results we have to calculate the $C_I(V_I)$ curves for various values of C_H and let the potential scales slide on each other until a satisfactory fit is obtained. The value deduced for V_{FB} can then be compared with that obtained from a Schottky-Mott plot.

This comparison has been done for several experimental curves. Figure 9 results from a new interface with $C_H = 0.22$ F m^{-2}. The curves fit well in the -0.5 to -1.5 V region. Beyond -1.5 V the curves diverge and the discrepancy is about 20% at -2.5 V. The flat-band potential deduced from this fit always agrees with that deduced from the Schottky-Mott plot with a maximum

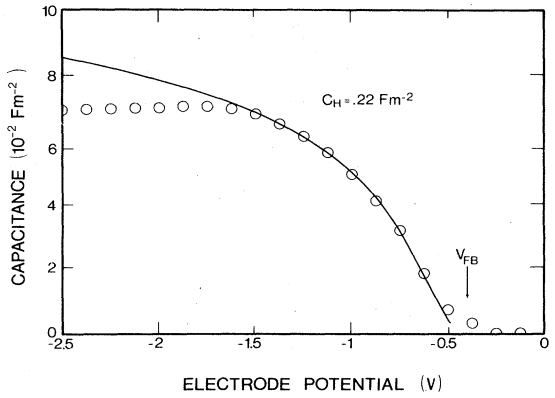

FIG. 9. Theoretical and experimental capacitance per unit surface of the (111) n-silicon/acetonitrile interface vs electrode potential. The fitting has been realized with a Helmholtz-layer capacitance of 0.22 F m^{-2}. V_{FB}, flat-band potential. The experimental curve has been obtained on a new interface.

discrepancy of 50 mV. The flat-band potential deduced from these experiments is -480 mV relative to the Ag/Ag$^+$ ($10^{-2}M$) reference. Then the conduction-band potential is -730 mV relative to the same reference, which is compatible with the value published by Chazalviel and Truong.[3] In order to test the significance of the fit we tried to fit a curve obtained by dividing by 2 the experimental values of the capacitance. This is equivalent to assuming a factor of surface roughness of 2. In these conditions, no satisfactory fit could be realized for any value of C_H and V_{FB}. We regard this fact as support for the significance of the fit and the hypothesis of negligible surface roughness. In the 0 to -0.5 V and -1.5 to -2.5 V potential regions, no satisfactory fit could be realized for any curves; therefore, some hypotheses must be reexamined.

The existence of surface states in the gap of silicon is probably sufficient to explain the discrepancy in the 0 to -0.5 V region. On the other hand, in the -1.5 to -2.5 V region, several hypotheses can be suggested:

(i) For electronic densities as high as 5×10^{13} cm^{-2}, the effective-mass approximation begins to be improper because the parallel and perpendicular electronic wave vectors $k_{\parallel}$ and $k_{\perp}$ reach about 10% of the dimension of the Brillouin zone.

(ii) In the same way, the validity of the relative permittivity $\epsilon_r = 11.7$ at 10 Å from the surface is doubtful. According to our estimate based on the published expression of a nonlocal permittivity,[12] the breaking of translational invariance due to the presence of the surface does not introduce major corrections. On the other hand, we have estimated the electrostatic energy of accumulated electrons, with a wave-vector-dependent permittivity.[13] We note that for $n_s = 5 \times 10^{13}$ cm^{-2} the result differs by 10% from that obtained with the value $\epsilon(q = 0)$.

(iii) The capacitance C_H of the Helmholtz layer depends on the accumulated charge. In the case of Fig. 9, a variation of 30% of C_H is sufficient to explain the discrepancy between theory and experiment at -2.5 V. Although we cannot assert that this variation actually ex-

ists in the case of the silicon/acetonitrile interface, it is quite likely, because such variations occur in similar systems for comparable surface charge densities.[14]

We think that the latter point is largely responsible for the discrepancy between theory and experiment, and because of two reasons: The capacitance of the interface may be rather insensitive to the variations of effective mass and permittivity, whereas it is directly affected by a variation of C_H. On the other hand, the discrepancy between the two curves appears rather abruptly, whereas we expect the correction due to the variation of effective mass and permittivity to depend more smoothly upon n_s.

The capacitance of the Helmholtz layer seems to be also affected by the evolution of the silicon surface. We have fitted an experimental curve obtained with an interface more than 1 d old. The agreement and the discrepancy between experimental and theoretical curves occur in the same regions as above, but the Helmholtz capacitance is found to be $C_H = 12\ \mu\text{F/cm}^2$ instead of $22\ \mu\text{F/cm}^2$ previously. The surface-state density has increased to $5.2\times10^{12}\ \text{cm}^{-2}$, but is still 1 order of magnitude smaller than the total electron density.

B. Electron mobility in the accumulation layer

The above discussion shows that C-V measurements are a reliable technique for the determination of the electron density versus electrode potential. Hence, having performed on an interface a C-V measurement and a conductivity (σ_{acc}) voltage measurement, we can derive a mobility (μ) versus electronic density curve, according to the relation $\sigma_{acc} = n_s e \mu$. Figure 10 shows the mobility versus electron density for four different experiments, together with the experimental results obtained by Sato for an inversion layer on a (111) face of monocrystalline silicon at room temperature.[15] We see, as expected, that the mobility decreases with increasing electron density. For $n_s \sim 5\times10^{13}\ \text{cm}^{-2}$ we find $\mu \sim 60\ \text{cm}^2/\text{V s}$, i.e., $\tau \sim 10^{-14}$ s. Two regions can be distinguished among our experimental points: above $2.5\times10^{13}\ \text{cm}^{-2}$ all the points tend to line up together on a straight line with slope $-\frac{1}{2}$. Below $2.5\times10^{13}\ \text{cm}^{-2}$ the points are more scattered and the curves bend but stay below the above line. A mobility of $60\ \text{cm}^2/\text{V s}$ for an electron density of $5\times10^{13}\ \text{cm}^{-2}$ is 25 times lower than the bulk mobility in silicon.[10] The mechanism responsible for this mobility drop must be very efficient. In MOS structures, phonon scattering is known to be an efficient scattering mechanism at room temperature and high electronic densities. The mobility limited by phonon scattering is also known to vary between $n_s^{-1/3}$ and $n_s^{-1/6}$ according to crystal orientation and for $5\times10^{11} < n_s < 5\times10^{12}\ \text{cm}^{-2}$.[16] However, the theory of phonon scattering is not yet satisfactory, as the models generally predict mobilities too high by almost 1 order of magnitude. For $n_s \geq 10^{12}\ \text{cm}^{-2}$ there is no major difference between electron accumulation and inversion layers. Then we have compared our results with those of Sato on inversion layers. We see on Fig. 10 that the above-mentioned line with a slope of $-\frac{1}{2}$ also goes through the experimental points corresponding to the highest densities obtained by Sato. In the experiment of Sato the mobility is limited by phonon scattering, and we then think that, in our case, and for electronic densities higher than $2.5\times10^{13}\ \text{cm}^{-2}$, the mobility is limited by phonon scattering, although the slope of $-\frac{1}{2}$ is steeper than expected.

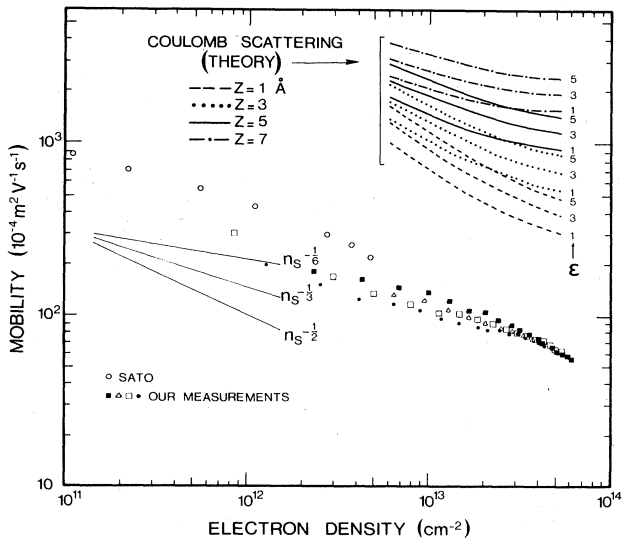

FIG. 10. Calculated and experimental curves of electron mobility on a (111) n-silicon/acetonitrile interface vs electron density. Our measurements correspond to an accumulation layer and Sato's measurements to an inversion layer. The calculated curves are for Coulomb scattering. Z, distance of charged centers from the surface; ϵ, permittivity of the Helmholtz layer.

In the region $n_s < 2.5\times10^{13}\ \text{cm}^{-2}$ our experimental point always stay below Sato's experimental points. This suggests that another scattering mechanism becomes dominant. According to Fig. 10 we estimate that the mobility limited by this other mechanism is in the (250—600)-$\text{cm}^2/\text{V s}$ range. The spreading of the experimental points may have two causes. The first one is the loss in accuracy since each point is the ratio of two small quantities: conductivity and electron density. Another cause is that in this region the mobility is more sensitive to the state of the surface that may differ from one experiment to another.

Three mechanisms may contribute to limiting the mobility in this region of accumulation: surface roughness, trapping of electrons in surface states, and Coulomb scattering.

(i) Surface-roughness scattering is known to be an efficient mechanism at high electronic densities. A mobility limited by surface roughness varies as n_s^{-2},[16] which corresponds to a straight line with a slope of -2 in Fig. 10. The experimental curves do not show such a variation. We take this as an indication of a weak surface roughness, which is in agreement with our conclusion of Sec. VI A.

(ii) The effect of electron trapping in surface states is difficult to estimate. In a first approximation this mechanism may induce an overvaluation of the mobile electron density, which may be important for densities of about $10^{12}\ \text{cm}^{-2}$.

(iii) Coulomb scattering might be especially important at the semiconductor/electrolyte interface. The presence, at a few angstroms from the surface, of a very high densi-

ty of positive ions (equal to the electronic density) induces Coulomb potentials that scatter the electrons of the accumulation layer. It is possible to calculate the mobility limited by Coulomb scattering with the theory due to Stern and Howard.[17] For this calculation we consider ions lying at a distance Z from the interface, in a medium of permittivity ϵ corresponding to the Helmholtz layer. This permittivity cannot be taken as the static permittivity of acetonitrile. In addition, the distance Z is not known. For example, in the case of water the permittivity is 80 and the permittivity of the Helmholtz layer is about 6.[18] We think this is also a correct order of magnitude in our case. The average distance Z is of a few interatomic distances, because the Debye length for an ionic concentration of $0.1M$ is $1.1\epsilon^{1/2}$ Å. Moreover, the capacitance C_H of the Helmholtz layer deduced from our measurements is about 20 μF/cm^2. We must have roughly $C_H=\epsilon_0\epsilon/Z=20$ μF/cm^2. The values $\epsilon=6$ and $Z=3$ Å are then plausible. Nevertheless, we made the calculations for several values of n_s, ϵ, and Z. The hypotheses that we used are the following. (i) Neglect of the anisotropy of the effective-mass tensor. The isotropic effective mass is taken as the density-of-states effective mass. (ii) Calculation using the first Born approximation, and, in particular, neglect of multiple scattering. (iii) Screening effect taken into account within the linear approximation. (iv) Only the lowest subband is taken into account. (v) All the scattering centers lie at a distance Z from the interface. (vi) Neglect of intervalley scattering.

We see in Fig. 10 that, even for small (hence unlikely) values of Z and ϵ, experimental and calculated curves still differ by almost an order of magnitude. A variant of this calculation allows an estimate of the mobility limited by the scattering by dipoles, corresponding to the molecules of acetonitrile in contact with the surface. This calculation seems to show that this latter mechanism is still less efficient than the scattering by ions. A more elaborate model would probably give weaker mobilities, because the hypotheses that we used here are near the limit of validity. We still consider it unlikely that Coulomb scattering accounts for the mobility at very high accumulations (more than 2.5×10^{13} cm^{-2}) where phonon scattering is the best candidate. Nevertheless, Coulomb scattering may account for a mobility of 250–600 cm^2/V s, and may dominate for accumulations below 2.5×10^{13} cm^{-2}.

A final remark can be made on the smallness of the scattering time. Because of the existence of a finite scattering time τ, the electronic levels are broadened, with $\Delta E\sim\hbar/\tau$. For $\tau=10^{-14}$ s, we have $\Delta E\sim65$ meV. The broadening of the electronic levels being larger than the value of the Fermi energy, the properties of the electron gas are modified, and, especially, the density of states in the accumulation layer is no longer independent of electron energy.[19] However, in view of the satisfactory agreement between theory and experiment, we did not estimate the effects of these facts on the calculation presented in Sec. V.

C. Optical absorption by the accumulation layer

The optical absorption of free electrons in accumulation layers has been studied by several authors, and a λ^2 dependence of the absorption, where λ is the wavelength, has sometimes been reported.[20,21] We, however, observed instead a $\lambda^{3/2}$ variation between 1.1 and 10 μm. The relative absorption that we observe is much larger than those published for similar experiments,[20,21] but always stays much smaller than 1. Therefore we can find an expression for it using a perturbation method, i.e., we calculate the electric field E of the light beam in the absence of accumulation layer, and then calculate the relative absorbed power A_s and A_p for the two polarizations s and p, respectively (using $\sigma E^2/2$), assuming that the accumulation layer has complex parallel and perpendicular conductivities $\sigma_{||}(\omega)$ and $\sigma_\perp(\omega)$, respectively. The free motion of electrons in the plane of the layer is described by $\sigma_{||}(\omega)$, whereas $\sigma_\perp(\omega)$ is related to the polarizability and intersubband transitions. We find

$$A_s=\frac{4n_1\cos i}{(n_1^2-n_2^2)\epsilon_0 c}\alpha(\omega) \tag{1}$$

and

$$\frac{A_p}{A_s}=\frac{(n_1^2-n_2^2)\,|\cos i_2\,|^2}{(n_1^2\,|\cos i_2\,|^2+n_2^2\,|\cos i_1\,|^2)}\times\left[1+\frac{n_2^2\sin^2 i_1}{n_1^2\,|\cos i_2\,|^2}\xi(\omega)\right],$$

with n_1 the optical index of silicon, n_2, the optical index of acetonitrile, i_1, the angle of incidence, and i_2 the refracted angle (complex for attenuated reflection spectroscopy). We also have

$$\alpha(\omega)=\int_z \mathrm{Re}(\sigma_{||})dz \quad\text{and}\quad \int_z \mathrm{Re}(\sigma_\perp)dz=\xi(\omega)\alpha(\omega)\,. \tag{2}$$

In our case, $i_1=45°$, $n_1=3.4$, and $n_2=1.34$, and then we have

$$A_P/A_s=0.82[1+0.034\xi(\omega)]\,.$$

This expression is in good agreement with our measurement, provided $\xi(\omega)$ is at most of order 1. The intersubband transitions described by $\xi(\omega)$ might induce some structure in the absorption spectrum, but this was not observed because of two reasons: (i) the difference of index between silicon and acetronitrile allows only a weak perpendicular electric field inside silicon in our geometry, and (ii) according to a previous remark, the scattering time is so short that the absorption lines would be very broad. Within the framework of the Drude model, we have

$$\alpha(\omega)=\frac{n_s e^2}{m^*}\left\langle\frac{\tau}{1+\omega^2\tau^2}\right\rangle,$$

where the angular brackets stand for energy averaging.[16] Then A_s can be expressed as

$$A_s=Kn_s\left\langle\frac{\tau}{1+\omega^2\tau^2}\right\rangle,$$

where K only depends on geometry and fundamental constants.

If we assume that the phonon scattering time τ is almost independent of electron energy, then we have

$$A_s \sim K \frac{n_s \tau}{1+\omega^2\tau^2} .$$

This is a Lorentzian curve. A_s varies as ω^{-2} at high frequencies instead of $\omega^{-3/2}$ in our experiment: We cannot fit our experimental curve with this expression.

We can fit our results with the sum of two Lorentzian curves, $\tau_1 = 2\times10^{-15}$ s and $\tau_2 = 1.2\times10^{-14}$ s, while constraining n_s and $\langle\tau\rangle$ to the experimental values: $n_s = 5.4\times10^{13}$ cm^{-2} and $\langle\tau\rangle = 10^{-14}$ s. However, this fit lacks any physical support. We could also fit our experimental curve by assuming simultaneously two scattering mechanisms, e.g., phonon scattering and Coulomb scattering. We took $\tau = \tau_0$ independent of electron energy for phonon scattering and $\tau = A\epsilon^\alpha$ for Coulomb scattering. τ_0, A, and α were taken as fitting parameters. This fit is not very satisfactory either because the obtained fitting parameters are not realistic. In particular, the exponent α must have a value of about 3. Therefore no satisfactory fitting could be found within the framework of the Drude model.

However, Fan, Spitzer, and Collins developed a theory valid for free-carrier absorption in bulk germanium, and they justly found a $\omega^{-3/2}$ variation.[22] Briefly, optical absorption cannot be described by the Drude model if the energy $\hbar\omega$ of the incident photons is not much smaller than thermal energy kT. In this case, which corresponds to ours, electrons are promoted very high in the conduction band, and electron-phonon interaction must be more properly treated. In the case where $kT \ll \hbar\omega$, they find

$$\sigma(\omega) = \frac{4}{9\pi^{1/2}} \frac{\sigma_0}{\tau^2\omega^2} \left[\frac{\hbar\omega}{kT}\right]^{1/2} , \tag{3}$$

where $\sigma_0 = n_v e^2 \tau_v / m^*$.

We can easily understand this result. For a three-dimensional electron gas and within the framework of the Drude model, we have

$$\sigma(\omega) = \frac{n_v e^2}{m^*} \left\langle \frac{\tau(\epsilon)}{1+\omega^2\tau^2(\epsilon)} \right\rangle .$$

If $\hbar\omega$ is of the order of kT, τ also depends on ω; if $\hbar\omega$ is much larger than kT, it practically depends on ω alone:

$$\sigma(\omega) = \frac{n_v e^2}{m^*} \frac{\tau(\omega)}{1+\omega^2\tau^2(\omega)} .$$

Now, for electron-phonon interaction, $1/\tau$ is proportional to the final density of states at the final energy $\epsilon+\hbar\omega \sim \hbar\omega$. Then, $1/\tau$ is nearly proportional to $\omega^{1/2}$. For $\omega\tau \gg 1$ we then have $\sigma(\omega) = K\omega^{-3/2}$.

It is reasonable to think that this model is valid in our case at very high frequencies, because even if electrons are initially confined near the surface, they are excited very high in the conduction band, where they are no longer confined. However, our measurements give $A_s = C\omega^{-3/2}$ with $C = 1.45\times10^{23}$ s$^{-3/2}$ in all of the spectral region that we investigated, and the value of the constant C, calculated from Eqs. (1)—(3), differs by less than 20% from this value. It is difficult to decide whether the quantitative agreement between this model and our results is only a coincidence, because the matrix elements in our case involve confined and nonconfined electronic states and are therefore not straightforward to evaluate.

According to this discussion, we think that electron-phonon interaction is responsible for the intensity and shape of optical absorption. A way to test this conclusion would be the measurement of the mobility versus temperature because it is known to vary as T^{-1}.[16] This investigation is practically impossible to perform on the silicon/liquid electrolyte interface for lower temperatures. However, it could be made on a silicon/superionic conductor interface. We have made a preliminary experiment at room temperature with a silicon/HUP (hydrogen uranyl phosphate) interface. HUP is one of the best superionic conductors known, with a room-temperature conductivity of $\sim6\times10^{-3}$ Ω^{-1} cm^{-1}.[23] Comparable and even higher accumulations than those mentioned above seem to be feasible with this interface.

We would like to make a final remark concerning the possibility to realize inversion layers at the n-silicon/acetonitrile interface. As stated in Sec. II, a thick depletion layer is realized by applying positive potentials. The possibility of sustaining an inversion layer at the surface depends upon the competition between hole generation in the semiconductor and hole transfer to the electrolyte. On the basis of capacitance measurements, some authors claimed that an inversion layer is indeed present.[24,25] We, however, found that in our experimental conditions no evidence for such a layer could be obtained either from capacitance measurements or from the infrared absorption.

VII. CONCLUSION

We have demonstrated that it is possible to create very high electronic concentrations at the surface of (111)-oriented monocrystalline silicon, up to 8×10^{13} cm^{-2} with the silicon/(acetonitrile + 0.1M tetrabutylammonium perchlorate) interface. We have extended the existing theory to the case of highly concentrated accumulation layers and we find satisfactory agreement with our experimental results. The comparison between theory and experiment allows deduction of a value of 0.22 F cm^{-2} for the capacitance of the Helmholtz layer, and a flat-band potential in good agreement with that determined from a Schottky-Mott plot. The mobility of electrons in the accumulation layer is determined as a function of electron density. It varies as $\sim n_s^{-1/2}$ at very high concentrations. From comparison with earlier work done on silicon MOSFET's (MOS field-effect transistors), it can reasonably be assumed to be limited by phonon scattering. The problem of Coulomb scattering has been investigated, but this mechanism seems to be unimportant at very high concentrations. We present the measurement of optical absorp-

tion of the accumulation layer in the (1.1—10)—μm spectral region, by the attenuated-total-reflection technique. This absorption is about 4% per reflection at 10 μm and varies as $\omega^{-3/2}$. This is compatible with the theory of Fan *et al.* and a phonon scattering mechanism. A preliminary experiment using a superionic conductor suggests that it might be possible to test the validity of this conclusion at low temperatures.

ACKNOWLEDGMENTS

We are indebted to B. Vinter for many extremely valuable discussions. We are also grateful to J. P. Badiali, R. Parsons, and F. Abeles for stimulating discussions, P. Colomban for the realization of the HUP/silicon interface, and J. Harrang and C. Hermann for a critical reading of the manuscript. Part of this work was supported by Thomson-CSF.

*Present address: Laboratoire Central de Recherches, Thomson-CSF, Corbeville, Boîte Postale No. 10, F-91401 Orsay (Cédex), France.

†Groupe de Recherche No. 050038 du Centre National de la Recherche Scientifique.

[1]T. Ando, A. B. Fowler, and F. Stern, Rev. Mod. Phys. **54**, 437 (1982).

[2]D. T. Sawyer and J. L. Roberts, Jr., *Experimental Electrochemistry for Chemists* (Wiley, New York, 1974), p. 208.

[3]J.-N. Chazalviel and T. B. Truong, J. Am. Chem. Soc. **103**, 7447 (1981).

[4]N. J. Harrick and K. H. Beckmann, in *Characterization of Solid Surfaces,* edited by P. F. Kane and G. R. Larrabee (Plenum, New York, 1974), p. 215.

[5]J. Regh and G. A. Silvery, Electrochem. Technol. **6**, 155 (1968).

[6]D. T. Sawyer and J. L. Roberts, Jr., *Experimental Electrochemistry for Chemists,* Ref. 2, p. 259.

[7]I. Ikezawa and M. Ishigame, J. Phys. Soc. Jpn. **50**, 3734 (1981).

[8]M. J. Madou, B. H. Loo, K. W. Frese, and R. Morrison, Surf. Sci. **108**, 135 (1981).

[9]See Ref. 1, Sec. III.

[10]S. M. Sze, *Physics of Semiconductor Devices* (Wiley-Interscience, New York, 1969).

[11]See Ref. 1, Sec. II.

[12]D. I. Sheka and A. M. Voskovoinikov, Fiz. Tverd. Tela (Leningrad) **25**, 169 (1983) [Sov. Phys.—Solid State **25**, 92 (1983)].

[13]J. P. Walter and M. L. Cohen, Phys. Rev. B **2**, 1821 (1970).

[14]S. Trasatti, Mod. Aspects Electrochem. **13**, 181 (1979).

[15]T. Sato, Y. Takeishi, and H. Hara, Phys. Rev. B **4**, 1950 (1971).

[16]See Ref. 1, Sec. IV.

[17]F. Stern and W. E. Howard, Phys. Rev. **163**, 816 (1967).

[18]J. O'M. Bockris and A. K. N. Reddy, *Modern Electrochemistry* (Plenum, New York, 1970), Vol. 2, p. 757.

[19]T. Ando, J. Phys. Soc. Jpn. **51**, 3215 (1982).

[20]H. Gobrecht, A. de Haan, and R. Thull, Ber. Bunsenges. Phys. Chem. **76**, 602 (1972).

[21]N. J. Harrick, Phys. Rev. **125**, 1165 (1962).

[22]H. Y. Fan, W. Spitzer, and R. J. Collins, Phys. Rev. **101**, 566 (1956).

[23]A. T. Howe and H. G. Shilton, J. Solid State Chem. **34**, 149 (1980).

[24]J. A. Turner, J. Manassen, and A. J. Nozik, Appl. Phys. Lett. **37**, 488 (1980).

[25]E. Kamieniecki and G. Parsons, in *Proceedings of the 164th Meeting of the Electrochemical Society* (The Electrochemical Society, Washington, D.C., 1983), p. 561.